

Towards Class-Specific Unit

Runkai Zheng¹, Zhijia Yu², Yinqi Zhang¹, Chris Ding³, Hei Victor Cheng⁴, Li Liu^{5,*}

¹Department of Computer Science, Jinan University, Guangzhou, China

²Tsinghua University, Beijing, China

³ The Chinese University of Hong Kong Shenzhen, Shenzhen, China

⁴ Department of Electrical and Computer Engineering, University of Toronto, Toronto, Canada

⁵Shenzhen Research Institute of Big Data, Shenzhen, China

Abstract

Class selectivity is an attribute of a unit in deep neural networks, which characterizes the discriminative ability of units to a specific class. Intuitively, decisions made by several highly selective units are more interpretable since it is easier to be traced back to the origin while that made by complex combinations of lowly selective units are more difficult to interpret. In this work, we develop a novel way to directly train highly selective units, through which we are able to examine the performance of a network that only rely on highly selective units. Specifically, we train the network such that all the units in the penultimate layer only response to one specific class, which we named as class-specific unit. By innovatively formulating the problem using mutual information, we find that in such a case, the output of the model has a special form that all the probabilities over non-target classes are uniformly distributed. We then propose a minimax loss based on a game theoretic framework to achieve the goal. Nash equilibria are proved to exist and the outcome is consistent with our regularization objective. Experimental results show that the model trained with the proposed objective outperforms models trained with baseline objective among all the tasks we test. Our results shed light on the role of class-specific units by indicating that they can be directly used for decisions without relying on low selective units.

1. Introduction

Convolutional Neural Networks (CNNs) achieve a great success in computer vision. Commonly in image recognition, CNNs are used to map the input data to deep features by stacking convolutional layers with non-linear activation functions, then the linear classifier separates different categories on the feature space. Conventionally, Cross Entropy

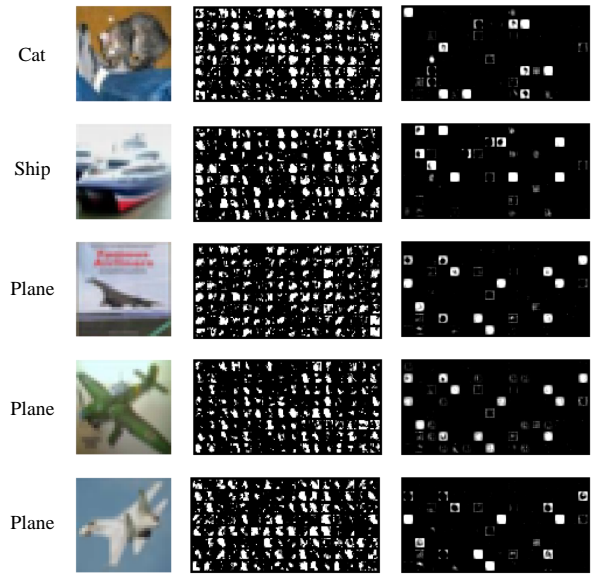


Figure 1. Motivation of our work. From the left to the right, the first column indicates the class of images. The second column shows the original input images. The third column shows the activations on the penultimate layer’s 128 feature maps on the standard CE trained CNN, where each map has 8 x 8 grids, and the fourth column shows activations of the same feature maps on our minimax-loss trained CNN. Clearly, our minimax-loss trained CNN generates a very sparse class-specific units (feature maps), and three different airplanes in “airplane” class generate very similar feature maps.

(CE) loss with softmax is used to train the network in an end-to-end manner.

Recent studies [15, 23, 25] showed that CNNs not only learns shallow features, but also encode highly selective concepts in individual units. The relationship between the class selectivity of a unit and its importance is still controversial [1, 17, 26]. These research works studied highly selective units that already exist in normally trained CNNs. In this work, we develop a novel way to directly train

*Corresponding author: liuli@cuhk.edu.cn

class-specific units, which provides a new perspective for analysing the effect of a single unit. Specifically, we train a network such that all the units in the penultimate layer only response to one specific class. This idea is illustrated in Fig. 1, last column, we want each class to have its own set of units that will only be activated when a particular class is seen. Objects belonging to the same class (*e.g.*, the planes in Fig. 1) share the same subset of units, while different classes (*e.g.*, the planes and the ship in Fig. 1) do not have shared units. Comparing with the CE trained units (see Fig. 1, second column) that learn general features activated for different classes, specialized units reduce similarity among classes to avoid misclassification. In other words, for a given image, we expect the penultimate layer units to be strongly correlated with the target class and uncorrelated with the non-target classes.

The behaviour of the penultimate layer’s feature map motivates us to design a novel regularizer to produce *class-specific units* in the penultimate layer. To achieve this goal, we formulate this problem using the Mutual Information (MI), from which we deduce an explicit regularization objective, *i.e.*, *Maximum Non-Target distribution Entropy (MaxNTE)*. To efficiently optimize the objective, we propose a game theoretic framework to simplify the problem formulation. Under this game theoretic framework, the existence of Nash equilibria and the consistency between the outcome and our objective are proved rigorously. On this basis, we arrive at a simple yet efficient final loss function to achieve the regularization goal formulated using MI. To evaluate the performance of our proposed method, extensive experiments are performed on different standard visual classification and the fine-grain visual classification (FGVC) tasks. Experimental results verify that our method achieves our goal of having highly selective units. Moreover, our method achieves comparable performances with other baseline method while promotes the selectivity of the units. Finally, our method also has the advantage of being model-agnostic and can be applied on arbitrary backbone models.

In summary, there are three main contributions of this work:

- 1) We propose a method to train a network such that the penultimate layer units are class-specific. To achieve the goal, a new regularizer is innovatively formulated from an information theoretic perspective. Under this theoretic framework, we find that the output of the model should have a special form that all the probabilities over non-target classes are uniformly distributed.

- 2) A minimax loss is proposed based on a game theoretic framework, where a game is formulated between the model and a designed adversary to efficiently achieve the regularization objective formulated using MI. To the best of the author’s knowledge, this is the first work that applies game theory to the object recognition task.

- 3) Experimental results on several influential benchmarks show the superiority of the proposed model, as well as the good generalization ability on different classification tasks. Besides, our results shed light on the role of class-specific units by indicating that class-specific units can be used for decisions independently of low selective units.

2. Related Work

Role of Individual Units Prior works have shown that individual units in CNNs are able to capture meaningful concepts [2, 23, 25]. It has been found that some individual units with high class selectivity play an important role as an object detector. To evaluate the importance of units with different class selectivity, unit ablation experiments were performed to show the influence of individual units to the network performance [17]. Counterintuitively, they found that class selectivity is a poor predictor of unit importance towards overall accuracy. Subsequently, another paper [26] shows that although eliminating highly selective units did not seem to affect the overall accuracy, it does impair the classification accuracy of the relevant categories. These conclusions drawn from ablation studies only apply to specific trained CNNs, and does not generalize to other networks. In contrast, we propose a method to directly trained a CNN to obtain class-specific units in the penultimate layer. The method is based on enforcing all the penultimate layer units to be class-specific by applying an explicit regularization goal to the output distribution.

Since all the penultimate layer units encode class-specific concepts, the final decision is made by the combination of these concepts. We draw an important conclusion from experimental results that class-specific units can be used for decisions independently of low selective units with better generalization.

Mutual Information is a measure of information in information theory, which provides a way to quantifies the mutual dependencies between two random variables. In deep learning, it was shown that Deep Neural Networks (DNNs) can be quantified by the MI between the layers and the input and output variables in [21]. They provide a novel perspective that the goal of DNNs is to optimize Information Bottleneck trade-off between compression and prediction. Rich knowledge about MI into the construction of encoder was explored in [12]. Belghazi et al. [3] proposed MI Neural Estimator and applied it to Generative Adversarial Networks (GANs) [10] to improve the reconstruction quality. To improve the quality of semantic segmentation, Region MI was investigated in [24] to compact the correlation of pixels within a region. MI plays an important role in our work, based on which we formulate our problem.

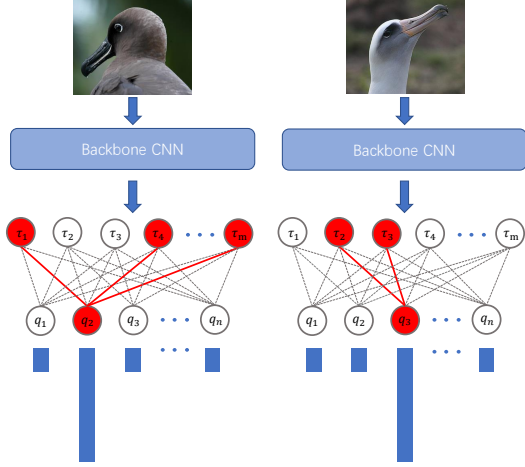


Figure 2. Ideal result of our approach. The red units are activated while the white units are turned off. For two images with different objects, they do not have shared units in the penultimate layer.

Game Theory provides a mathematical models of strategic interaction among intelligent decision makers [18]. It is a mathematical theory and method to study the phenomenon of competition, and was studied in [19] the interaction between the formulaic incentive structures. With the increasing popularity of Artificial Intelligent, game theory has been applied to different fields including Multi-Agent Reinforcement Learning [4] and GANs [10, 9]. In this work, we apply game theory to the object recognition task.

3. Method

To achieve the goal that each of the units in the penultimate layer encodes a class-specific concept, we first formulate the problem based on MI, and deduce a regularization objective, where a key finding is derived (*i.e.*, all output probabilities over non-target classes should be uniformly distributed). To efficiently optimize this objective function, we propose a minimax loss to simplify the reformulated regularization objective.

3.1. Mutual Information based Problem Formulation

We denote the input space by \mathcal{X} , the label space by $C = \{1, 2, \dots, n\}$, where $n > 2$ is the number of classes. The training data are all i.i.d sample pairs (x, y) , where y is in the form of a n -dimensional one-hot vector.

Let Φ be a parametric function mapping from the input space to the feature space. Ψ maps the feature to an n -dimensional logits $z \in \mathbb{R}^n$. Overall parameter set of the model is θ . Consider one of the **fix target categories** $t \in C$, and the corresponding input X^t (*i.e.*, images that belong to the class t). $\hat{Y}_{C \setminus t}$ is the predicted output of non-target classes with distribution $q_{C \setminus t} = \text{softmax}(z_{C \setminus t})$, where $z_{C \setminus t} = [z_1, z_2, \dots, z_{t-1}, z_{t+1}, \dots, z_n]$. Note that all the random variables y, z, q, t are dependent on input x , here

we omit the dependence for brevity.

Our goal is to train all the penultimate layer units to be class specific, that is, for a given image, we want to only activate the class-related units and turn off the other units (see Fig. 2). If we view the activation of each unit as a signal encoding some information related to a specific class, then for a given image of a class, the ideal activation of the penultimate layer units only contains information about that class, not about other non-target classes. MI serves this purpose as it is a measure to characterize the dependencies between different random variables. The problem formulation can be written as minimizing the MI between predicted output of non-target classes $\hat{Y}_{C \setminus t}$ and unit activation $\Phi(X^t)$, *i.e.* $I_\theta(\hat{Y}_{C \setminus t}; \Phi(X^t))$. However, this MI cannot be computed in practice as the distribution of $\Phi(X^t)$ is intractable. To resolve the intractability issue, we apply the data processing inequality [6] and use the obtained upper bound, the MI between input X^t of class t and predicted output of non-target classes $\hat{Y}_{C \setminus t}$, as our objective:

$$I_\theta(\hat{Y}_{C \setminus t}; X^t), \quad (1)$$

where $I_\theta(\hat{Y}_{C \setminus t}; X^t)$ represents the mutual information under model parameter θ .

According to the property of MI, *i.e.*, $I(A; B) = H(A) - H(A|B)$, where H is the entropy, and A, B are two random variables, Eq. 1 can be decomposed into the difference between entropy and conditional entropy:

$$I_\theta(\hat{Y}_{C \setminus t}; X^t) = H_\theta(\hat{Y}_{C \setminus t}) - H_\theta(\hat{Y}_{C \setminus t}|X^t), \quad (2)$$

where $H_\theta(\cdot)$ denotes the entropy under model parameter θ . Computing $H_\theta(\hat{Y}_{C \setminus t})$ involves the marginalization over X^t which is computationally intractable in practice. Thus, instead of directly optimizing Eq. 1, we consider optimizing its upper bound. From the fact that entropy reaches its upper bound when all the probabilities are equal, we have:

$$H_\theta(\hat{Y}_{C \setminus t}) \leq -(n-1) \frac{1}{n-1} \log \frac{1}{n-1} = \log(n-1),$$

The following lemma gives a theoretic justification for using the upper bound to replace Eq. 1.

Lemma 1. *When the conditional probability distribution over non-target classes is uniform, the MI in Eq. 1 is 0, and hence $I_\theta(\hat{Y}_{C \setminus t}; \Phi(X^t)) = 0$.*

Proof. From previous discussions, we have

$$I_\theta(\hat{Y}_{C \setminus t}; X^t) \leq \log(n-1) - H_\theta(\hat{Y}_{C \setminus t}|X^t). \quad (3)$$

On the other hand, when the conditional probability distribution over non-target classes is uniform, we have

$$H_\theta(\hat{Y}_{C \setminus t}|X^t) = \log(n-1).$$

Therefore $I_\theta(\hat{Y}_{C \setminus t}; X^t) \leq 0$, combining with the fact that MI is always non-negative gives $I_\theta(\hat{Y}_{C \setminus t}; X^t) = 0$. Finally we have $I_\theta(\hat{Y}_{C \setminus t}; \Phi(X^t)) \leq I_\theta(\hat{Y}_{C \setminus t}; X^t) = 0$, and thus $I_\theta(\hat{Y}_{C \setminus t}; \Phi(X^t)) = 0$. \square

Lemma 1 shows that making the conditional distribution of the non-target classes uniform is desired. Thus we formulate the problem using the upper bound as maximizing $H_\theta(\hat{Y}_{C \setminus t}|X^t)$, which promotes the distribution to be uniform. When the mutual information is $I_\theta(\hat{Y}_{C \setminus t}; \Phi(X^t)) = 0$, this suggests that the activation of the penultimate layer contains no information about the non-target classes.

In practice, we maximize the empirical conditional entropy for each class t :

$$\frac{1}{N^t} \sum_{i=1}^{N_t} H_\theta(\hat{Y}_{C \setminus t}|x_i^t), \quad (4)$$

where N_t is the number of training samples in class t .

We use the empirical conditional entropy as a regularization term with a weight parameter λ into the CE objective function to form the overall objective function (i.e., **MaxNTE**):

$$\theta^* = \arg \min_{\theta} \mathbb{E}_{x \sim \mathcal{X}} [D_{CE}(y||q(x; \theta)) - \lambda H_\theta(\hat{Y}_{C \setminus t}|X^t)]. \quad (5)$$

Here, $H_\theta(\hat{Y}_{C \setminus t}|X^t)$ has a reachable upper bound. However, directly taking this as the objective function may not be the best choice for our goal, since the gradients become extremely small when closing to the upper bound. From Lemma 1, we know a sufficient condition for $I_\theta(\hat{Y}_{C \setminus t}; \Phi(X^t)) = 0$ is to enforce the conditional distribution of non-target class to be uniform. In the following, we propose an efficient minimax loss based on game theory to achieve this target, which is lightweight and also insensitive to the hyper-parameter. The comparison of MaxNTE and our proposed loss will be provided in the experiments.

3.2. Game Theoretic Framework

In this section, we introduce the game theoretic framework in detail. The final loss function will be shown in Eq. 6, which is used as our main method in the experiments.

3.2.1 Preliminaries

Here we introduce some basic game-theoretic definitions that we will use later.

Definition 1. A strategic game is a tuple $G = \langle I, (A_i)_{i \in I}, (u_i)_{i \in I} \rangle$, where I is a nonempty set of players, A_i is the set of actions available to each player $i \in I$, $A = \prod_{i \in I} A_i$ is the profiles of actions and $u_i : A \rightarrow \mathbb{R}$ defines the payoff function for each player $i \in I$. A two player

strictly competitive game or zero-sum game is the strategic game G with $I = \{1, 2\}$ and for all $a \in A$:

$$u_1(a) = -u_2(a).$$

Definition 2. A mixed strategy set S_i is the set of all probability distributions over A_i . $s_i \in S_i$ defines a mixed strategy for each player $i \in I$, and $s_i(a_i)$ is the probability that player i plays $a_i \in A_i$. In a two player game, the expected payoff of player i playing a mixed strategy against pure strategy can be calculated as:

$$U_i(s) = \sum_{a_i} s_i(a_i) u_i(a_i, a_{-i}).$$

Likewise, the expected payoff of playing a pure strategy against mixed strategy can be calculated as:

$$U_i(s) = \sum_{a_{-i}} s_{-i}(a_{-i}) u_i(a_i, a_{-i}),$$

where $-i$ denotes the players other than i .

Definition 3. Let G be the strategic game, $i \in I$ be a player, and $s_{-i} \in S_{-i}$ be a strategy profile of players other than i . Then a strategy $s_i^* \in S_i$ is a best response of player i to s_{-i} if:

$$\forall s_i \in S_i, U_i(s_i^*, s_{-i}) \geq U_i(s_i, s_{-i}).$$

Definition 4. A Nash equilibrium of the strategic game G is a action profile $s^* \in S$ such that for every player i , s_i^* is the best response to s_{-i}^* .

3.2.2 $p - q$ zero-sum strategic game

We define a zero-sum strategic game played between the model and a designed adversary with loss of the model defined as $D_{CE}(p||q)$. We let p be the ground truth label vector, normally one-hot encoding, while in our work we specifically design it for the objective. Here, p is the strategy of the adversary and q is the strategy of the model. We assume that the model is a classifier with confidence q_t on the target class. The model aims to assign the rest of the probability $1 - q_t$ to non-target classes to minimize the loss. The adversary is the controller of the ground truth with fixed p_t for the target class, and it aims to maximize the loss via adjusting the distribution on non-target class of p . This is a dynamic game that the two players play in order, in which the model goes first, and the adversary can adjust the strategy according to the previous action of the model.

Definition 5. For $p_t, q_t \in (0, 1)$, the defined strategic game

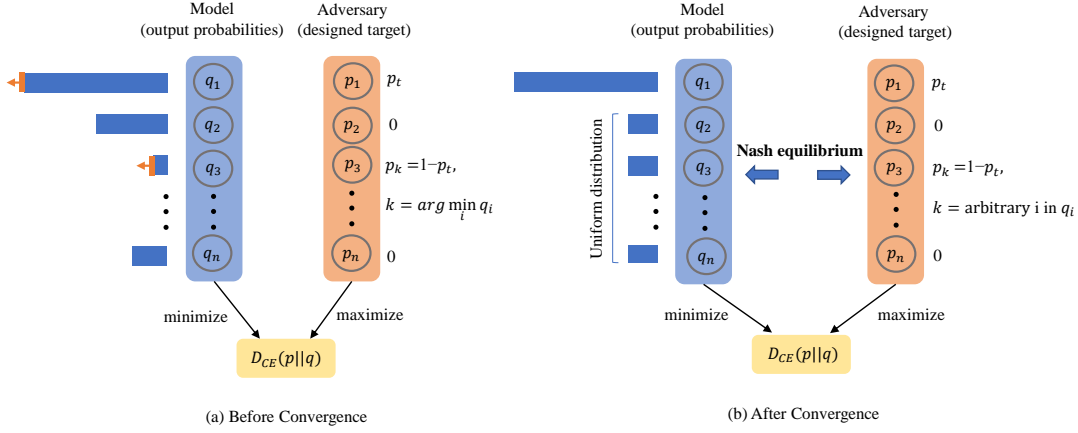


Figure 3. (a) During the training phase (before convergence), the model keep promoting the smallest probability in the non-target model output by assign $1 - p_t$ to the index of the minimum value in $q_{C \setminus t}$, i.e., q_3 in (a). (b) After iterations of training, the model output distribution will finally be uniformly distributed over non-target classes. When reaching a convergence, a Nash equilibrium exists between the optimal solution of the model and the adversary.

is a tuple $G = \langle (P, Q), (A_P, A_Q), (u_P, u_Q) \rangle$ with:

$$A_P = \{(p_i)_{1 \leq i \leq n}, p_i \in (0, 1), \sum_{i \neq t} p_i = 1 - p_t\}.$$

$$A_Q = \{(q_i)_{1 \leq i \leq n}, q_i \in (0, 1), \sum_{i \neq t} q_i = 1 - q_t\}.$$

$$u_P = D_{CE}(p||q) = -u_Q.$$

By Eq. 1, G is a two-player zero-sum game. In the following, we will prove the existence of Nash equilibrium in this game by giving the following three theorems.

Theorem 1. For $p_t, q_t \in (0, 1)$, we have:

$$\forall q \in A_Q, \quad p^* = \arg \max_p D_{CE}(p||q),$$

where $p^* = (p_i^*)_{1 \leq i \leq n}$:

$$p_i^* = \begin{cases} p_t, & i = t; \\ 1 - p_t, & i = k; \\ 0, & \text{otherwise} \end{cases},$$

for any $k = \arg \min_z (q_{C \setminus t})_z$.

Note that in the rest of the paper, if there exists more than one minimum value in $q_{C \setminus t}$, $k = \arg \min_z (q_{C \setminus t})_z$ refers to randomly taking one of them.

Proof. Since $k = \arg \min_z (q_{C \setminus t})_z$, then $\forall i \neq k, q_i \geq q_k$.

We have:

$$\begin{aligned} D_{CE}(p||q) &= - \sum_{i \neq k, t} p_i \log q_i - p_k \log q_k - p_t \log q_t \\ &\leq - \sum_{i \neq k, t} p_i \log q_k - p_k \log q_k - p_t \log q_t \\ &= - \left(\sum_{i \neq k, t} p_i + p_k \right) \log q_k - p_t \log q_t \\ &= -(1 - p_t) \log q_k - p_t \log q_t \\ &= D_{CE}(p^*||q), \end{aligned}$$

which concludes Theorem 1. \square

Theorem 2. For $p_t, q_t \in (0, 1)$, we have:

$$q^* = \arg \min_{q \in A_Q} D_{CE}(p^*||q),$$

where

$$q_i^* = \begin{cases} q_t, & i = t; \\ \frac{1 - q_t}{n - 1}, & \text{otherwise.} \end{cases}$$

Proof. Let $k = \arg \min_z (q_{C \setminus t})_z$. Since $\forall i \neq t, q_i^* = \frac{1 - q_t}{n - 1}$, for any $q \neq q^*$, we have $\forall i \neq t, q_i^* \geq q_k$:

$$\begin{aligned} D_{CE}(p^*||q) &= - \sum_i p_i^* \log q_i \\ &= -(1 - p_t) \log q_k - p_t \log q_t, \\ &\geq -(1 - p_t) \log q_i^* - p_t \log q_t, \\ &= D_{CE}(p^*||q^*), \end{aligned}$$

which concludes Theorem 2. \square

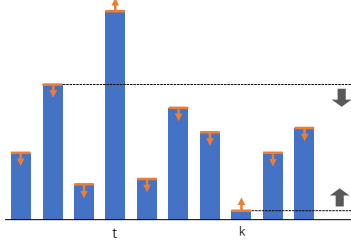


Figure 4. The minimax loss increases the target and minimum logits while reducing the remaining logits, indirectly minimizing the gap between the second largest logit and the minimum logit.

Theorem 1 actually gives the worst case payoff for the model q . However, since p^* depends on the index of the minimum value in q , they are not the best responses to each other. For example, when $q = q^*$, the adversary choose one of the indexes of the minimum values in q to determine p^* . Once p^* is fixed, q is no longer the best responses to p^* , since there exist a better q to get a higher payoff (e.g., change the position of the minimum value). Thus, we need randomize p to avoid this situation. Specifically, when $q = q^*$, the model uniformly distribute the probabilities over non-target classes. The adversary can randomly choose one of them since they are all the smallest value and the adversary’s strategy becomes a mixed strategy. In this case, the two strategies forms a Nash equilibrium. To show this mathematically, we gives the following theorem.

Theorem 3. Define an action subset for the adversary:

$$a_P^* \subset A_P = \left\{ (p_i) | p_i = \begin{cases} p_t, & i = t; \\ 1 - p_t, & i = k; \\ 0, & \text{otherwise} \end{cases} \right\},$$

where $k = \{1, 2, \dots, t-1, t+1, \dots, n\}$.

For the model:

$$a_Q^* = \left\{ (q_i) | q_i = \begin{cases} q_t, & i = t; \\ \frac{1-q_t}{n-1}, & \text{otherwise} \end{cases} \right\}.$$

Then we have the following strategies:

$$s_P^*(p) = \begin{cases} \frac{1}{n-1}, & p \in a_P^*; \\ 0, & \text{otherwise}. \end{cases}$$

$$s_Q^*(q) = \begin{cases} 1, & q \in a_Q^*; \\ 0, & \text{otherwise}, \end{cases}$$

such that $s^* = (s_P^*, s_Q^*)$ forms a Nash equilibrium.

The detailed proof of Theorem 3 is in Appendix.

3.2.3 Minimax Loss

The Nash equilibrium in a two player zero-sum game is equivalent to a minimax solution [8]. Thus, by training with the worst-case payoff $D_{CE}(p^* || q)$, we expect that the

model output ultimately converges to the best response q^* . Finally our proposed loss is defined as taking $D_{CE}(p^* || q)$ as the loss function:

$$\begin{aligned} \theta^* &= \arg \min_{\theta} \mathbb{E}_{x \sim \mathcal{X}} [D_{CE}(p^* || q)] \\ &= \arg \min_{\theta} \mathbb{E}_{x \sim \mathcal{X}} [-p_t \log q(x; \theta)_t - (1 - p_t) \log q(x; \theta)_k], \end{aligned} \quad (6)$$

where $k = \arg \min_a (q_{C \setminus t})_a$. Here, we leave p_t as a hyper-parameter to weight the regularizer of the objective corresponding to the class t . When p_t is set to 1 for all classes, the loss function degrades to the standard CE loss.

The internal mechanism of the optimization process is actually minimizing the gap between the second largest logit and the minimum logit. Consider the gradient on i^{th} logit:

$$\frac{\partial \mathcal{L}_{minimax}}{\partial z_i} = \begin{cases} q_i - p_t, & i = t; \\ q_i - (1 - p_t), & i = k; \\ q_i, & \text{otherwise}, \end{cases} \quad (7)$$

which indicates that we are actually promoting the minimum logit and the target logit as well as reducing the rest of the logits when $q_t < p_t$ and $q_k < 1 - p_t$. As shown in Fig. 4, the minimax loss indirectly minimize the gap between the second largest logit and the minimum logit to force the non-target logits to be nearly the same. Thus the mutual information between the unit activation of the penultimate layer and the non-target classes is forced to be nearly zero, as a result the units tend to respond only to a specific class.

4. Experiments

4.1. Experimental Setup

Our experiments are performed on standard visual classification benchmarks: CIFAR-10 [14], CIFAR-100 [14], STL-10 [5] and FGVC benchmarks: CUB-200-2011 [22], FGVC-Aircraft [16], Stanford Cars [13]. Different methods are compared using ResNet18 [11] and VGGNet11 [20] as the backbone models. The statistics of six datasets and the implementation details are introduced in Appendix.

We first compare our proposed minimax loss with MaxNTE. Then we quantitatively compare our proposed method with different methods on standard visual classification as well as the FGVC. Finally we conduct case study and visualization to further show the effect of our method.

4.1.1 Comparison between MaxNTE and minimax loss

We compare the minimax loss with the MaxNTE that directly maximize the Eq. 5 on CIFAR-10 dataset. Note that when p_t set to 1 for all classes (i.e. $1 - p_t$ set to 0) and

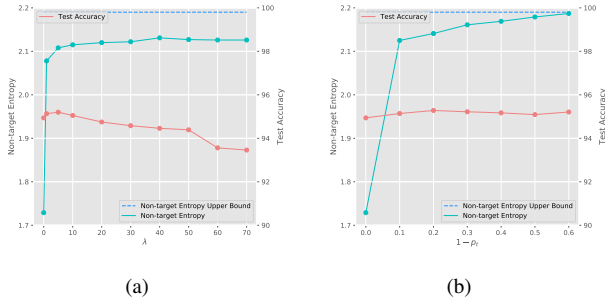


Figure 5. Comparison between minimax loss trained and MaxNTE loss trained models. Non-target classes entropy (scale using left vertical axis) and test accuracy (scale using right vertical axis) are shown. The entropy upper bound 2.197 is shown as the blue dotted line. We see that Minimax loss trained model reaches this upper bound, while MaxNTE trained model does not.

λ set to 0, both of the losses are equal to the cross entropy loss. In MaxNTE, as shown in Fig. 5, the left figure, the test accuracy is decreasing when λ is increasing, the maximum entropy reaches its bottleneck at about 2.12. The right figure shows that as $1 - p_t$ (hyperparameter) increases, the entropy gradually approaches its upper bound ($\log(n - 1) = \log 9 \approx 2.19$) with stable test accuracy. The results show that the minimax loss can achieve our goal in a better way, thus we apply it to the following experiments.

4.1.2 Quantitative results

Standard visual classification As shown in Table 1, our method outperforms several output regularization based methods across almost all the datasets and architectures. In CIFAR-10 and CIFAR-100, the improvements are not significant, and the test accuracy of VGGNet-11 with confidence penalty is slightly higher than that of our method in CIFAR-10. The case study in Fig. 6 shows how our method improves the classification of some hard examples. The images of cats and birds are considered the samples that near the classification boundary. The CE trained model misclassify the two images with close probabilities. Our model is able to precisely extract the different concepts from the two images rather than the similar features extracted by the CE trained model. In STL-10, our method outperforms three baselines by a large margin. It is worth mentioning that our method surpasses CE along all the settings, which indicates that high selectivity units can be used directly for classification tasks.

Backbone	Method	CIFAR-10	CIFAR-100	STL-10
VGGNet-11	Cross Entropy	92.26 \pm 0.08	70.37 \pm 0.33	79.80 \pm 0.31
	Confidence Penalty	92.62\pm0.05	70.30 \pm 0.19	80.17 \pm 0.14
	Label Smoothing	92.28 \pm 0.06	71.34 \pm 0.07	80.41 \pm 0.08
	Minimax Loss	92.43 \pm 0.06	71.62\pm0.18	82.26\pm0.09
ResNet-18	Cross Entropy	94.94 \pm 0.12	75.79 \pm 0.03	83.44 \pm 0.23
	Confidence Penalty	95.11 \pm 0.01	76.01 \pm 0.31	83.75 \pm 0.02
	Label Smoothing	95.08 \pm 0.11	76.24 \pm 0.21	84.03 \pm 0.01
	Minimax Loss	95.33\pm0.12	76.64\pm0.07	85.42\pm0.04

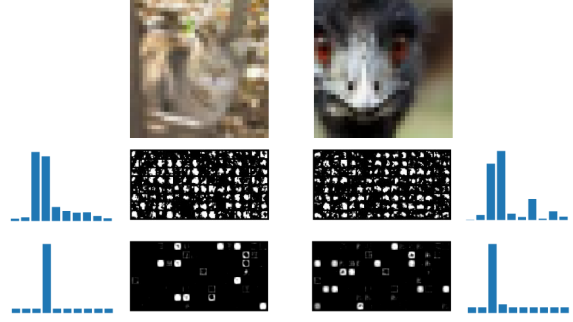


Figure 6. The first row shows the original images. The second and third row show the output probability distribution and penultimate layer feature maps generated by the CE trained model and the minimax trained model, respectively. The probabilities are obtained by scaling logits using softmax with temperature equal to 2 for better visualization. The minimax trained models have higher confidence by extracting distinctive features from the images.

cation independently of low selectivity units, and can even reach higher test accuracy. Compared with all the baselines, our method achieves better interpretability with competitive accuracy. The comparison of the unit selectivity of these methods is provided in the qualitative study.

Fine-grained visual classification We compare our method with SOTA regularization-based method in fine-grained visual classification tasks, *i.e.* MaxEnt [7]. MaxEnt maximize the entropy of the output distribution over all the classes, while ours only maximize that of the non-target distribution. From Table 2, our proposed minimax loss improves the performance of two baseline models trained with CE (*i.e.*, ResNet-18, VGGNet-11) in all three datasets (*i.e.*, CUB-200-2011, FGVC-Aircraft and Stanford Cars). Most notably, training VGGNet-11 with the minmax loss obtained a significant improvement of 3.71% on CUB. Moreover, our proposed method achieves comparable performance with MaxEnt across all the datasets and architectures we test. Our method actually train the model to identify different categories by several most discriminative regions detected by highly selective units. In fine-grained visual classification, finding the most discriminative features of different fine-grained categories is one of the most challenging problems. The qualitative analysis is provided in the next subsection.

Table 2. Comparison with regularization method on fine-grained visual classification tasks.

Backbone	Method	CUB	Aircraft	Stanford Cars
VGGNet-11	Cross Entropy	75.04 \pm 0.14	88.12 \pm 0.11	86.31 \pm 0.06
	MaxEnt ([7])	78.36 \pm 0.40	88.01 \pm 0.19	87.91\pm0.20
	Minimax Loss	78.75\pm0.33	88.68\pm0.16	87.72 \pm 0.15
ResNet-18	Cross Entropy	80.35 \pm 0.04	90.02 \pm 0.15	91.38 \pm 0.16
	MaxEnt ([7])	81.47 \pm 0.18	90.23 \pm 0.22	91.66 \pm 0.19
	Minimax Loss	81.68\pm0.14	90.61\pm0.22	91.72\pm0.09

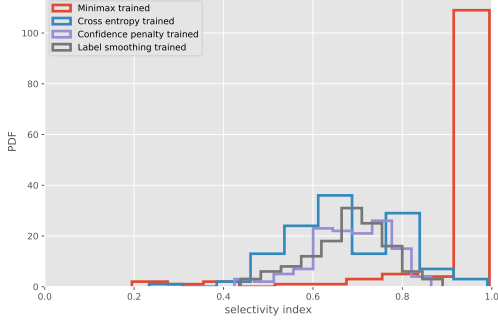


Figure 7. Distribution of selectivity of the units in the penultimate layer trained by different methods. Except for minimax, the other methods produce similar selectivity distribution that are relatively low. Minimax train the units to achieve almost the highest selectivity, which is consistent with our goal.

4.1.3 Qualitative results

Class Selectivity A neuroscience inspired index of class selectivity is introduced to measure the discriminability of classes of a single unit [17]:

$$selectivity = \frac{\mu_{max} - \mu_{-max}}{\mu_{max} + \mu_{-max}}, \quad (8)$$

where μ_{max} is the maximum mean activation across all the classes and μ_{-max} is the mean activation of all other classes. We calculate the selectivity index for each penultimate layer unit according to Eq. 8 and plot the probability density as shown in Fig. 7. The penultimate layer representations are high level representations, so the selectivity of those units are generally higher than that of the shallow layer. In this figure, they are mostly greater than 0.4. The distribution of selectivity indices for the units trained with three baseline loss did not differ significantly, ranging from 0.5 to 0.9, while the minimax trained units have selectivity distribution concentrate at around 1. In light of the above quantitative results, it may be beneficial to increase the penultimate layer unit selectivity to a higher level.

Representation Space To show how class-specific units make classification boundaries clearer, we visualize the penultimate layer representations by randomly picking samples from three classes of Stanford Car dataset and then scatter their representations on the basis of the top principle components, which is demonstrated in Fig. 8. We observed that in the second plot, all classes have obvious clustering trend even in the low dimensional space, which results in clearer classification boundary. On the other hand, CE relies more on low selective units, failed to learn discriminative representations to distinguish different fine-grained categories in such a low dimensional space.

Class Activation Maps We further visualize the network attention of the two models (CE trained and minimax

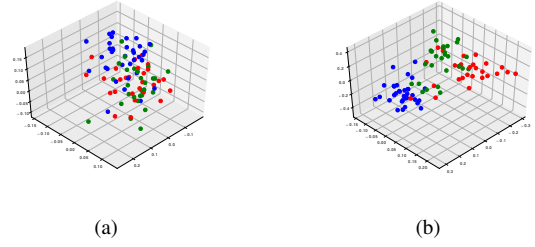


Figure 8. The penultimate layer feature representations of random samples on Stanford Cars dataset are projected to a 3-dimensional space. Three different colors represent three different classes. In such a low dimensional space, (a) the CE trained representations failed to cluster different fine-grained classes, while (b) the minimax trained representations result in a clearer classification boundary.

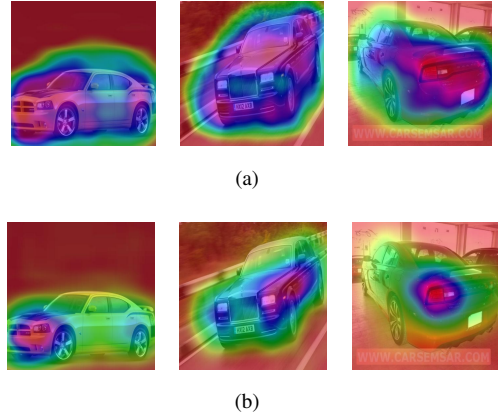


Figure 9. The class activation maps of random samples from Stanford Cars dataset demonstrate the differences of classification mechanism of the CE trained model (a) and the minimax trained model (b). The CE trained model generate complex combination of general features across the car body while the minimax trained one focus on the several discriminative parts.

trained) with random samples from Stanford Cars via Class Activation Mapping (CAM) [25] in Fig. 9. The activation maps show the discriminative image regions used by the CNN to identify that category. From the activation map, we can infer roughly how different trained networks make their decisions. Observing from the first row, the attentions of the CE trained model are distributed throughout the car body and the background, which indicates that the model identifies the cars using many different features, detected by low selective units, which are often noisy and difficult to interpret. The second row shows how class-specific units identifies different cars by their most discriminative parts. The class activation maps distinguish the differences of the classification mechanism of low selective units and high selective units. Regardless of the accuracy, the interpretability of the latter is better than that of the former.

5. Conclusion

To explore CNNs by analysing the role of individual units, this work focus on an extreme case that all the penultimate layer units are trained to be class specific. We innovatively formulate this idea from the perspective of Mutual Information, and deduce an explicit regularization objective MaxNTE for our goal. To efficiently achieve our regularization objective, a minimax loss is proposed based on a game theoretic framework between the model and a designed adversary. Experiments are performed on several influential benchmarks to demonstrate that class-specific units can be used for decisions independently of lowly selective units. Quantitative results show the superiority of our method compared to the baseline objective among all the tasks we test.

We provide a new perspective on analysing the highly selective units by direct training, and further investigations on the properties of class-specific units can be carried out on this basis. Moreover, this work reveals that the importance of a unit may not be simply explained by a single selectivity, its position in the network also matters, and there may be other more complex factors. One interesting extension of this work is to utilize the advantages of class-specific units in other research domains like multi-label classification and adversarial attack. We leave them for future work.

References

- [1] RA Amjad, K Liu, and BC Geiger. Understanding individual neuron importance using information theory. *IEEE Transactions on Neural Networks and Learning Systems*, 2019. 1
- [2] David Bau, Bolei Zhou, Aditya Khosla, Aude Oliva, and Antonio Torralba. Network dissection: Quantifying interpretability of deep visual representations. In *Proceedings of the IEEE conference on computer vision and pattern recognition*, pages 6541–6549, 2017. 2
- [3] Mohamed Ishmael Belghazi, Aristide Baratin, Sai Rajeshwar, Sherjil Ozair, Yoshua Bengio, Aaron Courville, and Devon Hjelm. Mutual information neural estimation. In *International Conference on Machine Learning*, pages 531–540, 2018. 2
- [4] Michael Bowling and Manuela Veloso. An analysis of stochastic game theory for multiagent reinforcement learning. 2000. 3
- [5] Adam Coates, Andrew Ng, and Honglak Lee. An analysis of single-layer networks in unsupervised feature learning. In *Proceedings of the fourteenth international conference on artificial intelligence and statistics*, pages 215–223, 2011. 6
- [6] Thomas M. Cover and Joy A. Thomas. *Elements of Information Theory*. John Wiley Sons, 2012. 3
- [7] Abhimanyu Dubey, Otkrist Gupta, Ramesh Raskar, and Nikhil Naik. Maximum-entropy fine grained classification. In *Advances in Neural Information Processing Systems*, pages 637–647, 2018. 7
- [8] Manuel Alberto M Ferreira, Marina Andrade, Maria Cristina Peixoto Matos, José António Filipe, and Manuel Pacheco Coelho. Minimax theorem and nash equilibrium. 2012. 6
- [9] Ian Goodfellow. Nips 2016 tutorial: Generative adversarial networks. *arXiv preprint arXiv:1701.00160*, 2016. 3
- [10] Ian Goodfellow, Jean Pouget-Abadie, Mehdi Mirza, Bing Xu, David Warde-Farley, Sherjil Ozair, Aaron Courville, and Yoshua Bengio. Generative adversarial nets. In *Advances in neural information processing systems*, pages 2672–2680, 2014. 2, 3
- [11] Kaiming He, Xiangyu Zhang, Shaoqing Ren, and Jian Sun. Deep residual learning for image recognition. In *Proceedings of the IEEE conference on computer vision and pattern recognition*, pages 770–778, 2016. 6
- [12] R Devon Hjelm, Alex Fedorov, Samuel Lavoie-Marchildon, Karan Grewal, Phil Bachman, Adam Trischler, and Yoshua Bengio. Learning deep representations by mutual information estimation and maximization. *arXiv preprint arXiv:1808.06670*, 2018. 2
- [13] Jonathan Krause, Michael Stark, Jia Deng, and Li Fei-Fei. 3d object representations for fine-grained categorization. In *4th International IEEE Workshop on 3D Representation and Recognition (3dRR-13)*, Sydney, Australia, 2013. 6
- [14] Alex Krizhevsky, Geoffrey Hinton, et al. Learning multiple layers of features from tiny images. 2009. 6
- [15] Aravindh Mahendran and Andrea Vedaldi. Understanding deep image representations by inverting them. In *Proceedings of the IEEE conference on computer vision and pattern recognition*, pages 5188–5196, 2015. 1
- [16] Subhansu Maji, Esa Rahtu, Juho Kannala, Matthew Blaschko, and Andrea Vedaldi. Fine-grained visual classification of aircraft. *arXiv preprint arXiv:1306.5151*, 2013. 6
- [17] Ari S Morcos, David GT Barrett, Neil C Rabinowitz, and Matthew Botvinick. On the importance of single directions for generalization. *arXiv preprint arXiv:1803.06959*, 2018. 1, 2, 8
- [18] R Myerson. *Game theory: Analysis of conflict* harvard univ. Press, Cambridge, 1991. 3
- [19] Martin J Osborne et al. *An introduction to game theory*, volume 3. Oxford university press New York, 2004. 3
- [20] Karen Simonyan and Andrew Zisserman. Very deep convolutional networks for large-scale image recognition. *arXiv preprint arXiv:1409.1556*, 2014. 6
- [21] Naftali Tishby and Noga Zaslavsky. Deep learning and the information bottleneck principle. In *2015 IEEE Information Theory Workshop (ITW)*, pages 1–5. IEEE, 2015. 2
- [22] Catherine Wah, Steve Branson, Peter Welinder, Pietro Perona, and Serge Belongie. The caltech-ucsd birds-200-2011 dataset. 2011. 6
- [23] Matthew D Zeiler and Rob Fergus. Visualizing and understanding convolutional networks. In *European conference on computer vision*, pages 818–833. Springer, 2014. 1, 2
- [24] Shuai Zhao, Yang Wang, Zheng Yang, and Deng Cai. Region mutual information loss for semantic segmentation. In *Advances in Neural Information Processing Systems*, pages 11115–11125, 2019. 2

- [25] Bolei Zhou, Aditya Khosla, Àgata Lapedriza, Aude Oliva, and Antonio Torralba. Object detectors emerge in deep scene cnns. In *ICLR*, 2015. 1, 2, 8
- [26] Bolei Zhou, Yiyou Sun, David Bau, and Antonio Torralba. Revisiting the importance of individual units in cnns via ablation. *arXiv preprint arXiv:1806.02891*, 2018. 1, 2